

Significant strain dependence of piezoelectric constants in $\text{In}_x\text{Ga}_{1-x}\text{N}/\text{GaN}$ quantum wells

G. Vaschenko, D. Patel, and C. S. Menoni

Department of Electrical and Computer Engineering, Colorado State University, Fort Collins, Colorado 80523-1373

N. F. Gardner, J. Sun, and W. Götz

LumiLeds Lighting, 370 W. Trimble Road, San Jose, California 95131

C. N. Tomé and B. Clausen

MST Division, Los Alamos National Laboratory, Los Alamos, New Mexico 87545

(Received 5 June 2001; revised manuscript received 17 October 2001; published 10 December 2001)

Using hydrostatic pressure to modify the strain in $\text{In}_x\text{Ga}_{1-x}\text{N}/\text{GaN}$ quantum wells we show an almost twofold increase of the built-in piezoelectric field in the wells from 1.4 MV/cm at atmospheric pressure to 2.6 MV/cm at 8.7 GPa. An analysis in terms of the total strain generated by the pressure suggests that the increase in the field arises from a significant dependence of the piezoelectric constants on strain.

DOI: 10.1103/PhysRevB.64.241308

PACS number(s): 77.65.Ly, 77.65.Bn, 78.66.Fd, 62.50.+p

Piezoelectric fields (F_{pz}) strongly affect the electrical and optical characteristics of GaN-based heterostructures with wurtzite lattice configuration. In light emitting devices specifically, piezoelectric fields are held responsible for the reduction in the emission efficiency and increase of the laser diode threshold current.¹ Recent calculations have shown that the F_{pz} in $\text{In}_x\text{Ga}_{1-x}\text{N}/\text{GaN}$ heterostructures could be as large as 1 MV/cm,¹ while values of the field obtained from experiments show a strikingly wide variation from 0.55 to 1.08 MV/cm for samples of similar geometry and composition.^{2,3} Quantifying the piezoelectric field in $\text{In}_x\text{Ga}_{1-x}\text{N}/\text{GaN}$ heterostructures requires the knowledge of the strain state, sample geometry, as well as piezoelectric constants. While the strains and sample geometry can be accurately determined, the piezoelectric constants are not generally known for the ternary compounds and are typically interpolated from binary constituents.^{1,4} This approach, however, ignores the effect that microscopic strains associated with alloy mixing and macroscopic strains produced by the lattice mismatch may have on these parameters.

Piezoelectric constants in semiconductors with wurtzite lattice configuration can be expressed in terms of the in-plane strain ε_{xx} (assumed to be equal to ε_{yy}), and the strain along the c axis, ε_{zz} as⁵

$$e_{31} = e_{31}^{(0)} + \frac{4eZ^*}{\sqrt{3}a_0^2} \frac{du}{d\varepsilon_{xx}}, \quad (1)$$

$$e_{33} = e_{33}^{(0)} + \frac{4eZ^*}{\sqrt{3}a_0^2} \frac{du}{d\varepsilon_{zz}}, \quad (2)$$

where $e_{31}^{(0)}$, $e_{33}^{(0)}$ are the clamped-ion terms that represent the effects of strain on the electronic structure, and the second term in Eqs. (1) and (2) is the contribution resulting from the relative displacement of the anion and cation sublattices (internal strain term). The other quantities in Eqs. (1) and (2) are the Born effective charge along the c axis, Z^* , the equilibrium lattice constant a_0 , and the internal parameter u [anion-cation bond length along the (0001) axis in units of c]. Shimada *et al.*⁶ evaluated the sensitivity of both the clamped-ion and internal strain terms to the applied strain in GaN, BN, and AlN for the specific case of deviatoric (vol-

ume conserving) strain.⁷ They predicted that in all of these materials the piezoelectric constants vary significantly with the deviatoric strain. In GaN, for example, e_{33} reduces from 0.63 C/m² at equilibrium to 0.23 C/m² at $\varepsilon_{zz}=0.02$, while e_{31} changes from -0.32 to -0.48 C/m² in the same strain range. As also shown in Ref. 6, the major contribution to the strain variation of e_{33} in GaN comes from the second term in Eq. (2), while e_{31} experiences comparable contributions from both terms in Eq. (1). This significant strain dependence of the piezoelectric constants in III nitrides is expected to produce strong nonlinear piezoelectric effect.^{6,8}

In this work we investigate the effect of macroscopic strain on the piezoelectric constants of $\text{In}_x\text{Ga}_{1-x}\text{N}/\text{GaN}$ quantum wells (QWs). We accomplish this by determining the magnitude of the piezoelectric field at different strain states generated by applying hydrostatic pressure (p). The signature of a nonlinear piezoelectric effect is obtained from the pressure rate of change of the photoluminescence (PL) peak energy (dE/dp), which decreases as the well width increases, and from the increase in the PL decay time. F_{pz} determined from the slope of the variation of the PL peak energy versus well width at each pressure is found to increase from 1.4 MV/cm at atmospheric pressure to 2.6 MV/cm at 8.7 GPa. Analysis of the pressure-induced strain suggests that this almost twofold increase in F_{pz} is due to changes in the piezoelectric constants with strain.

The QW structures studied in this work were grown by metal-organic chemical vapor deposition on (0001) sapphire substrates. Each sample has four identical quantum wells with indium composition of $\sim 15\%$, and well widths of 2.5, 3.1, and 3.8 nm, respectively. The barriers are GaN, 12.5 nm thick. The QW regions are grown on 3.5- μm GaN layers.

The PL was excited by the third harmonic of a mode-locked Ti:sapphire laser at 270 nm. The PL emission was collected in a backscattering geometry and detected with a 0.25 m spectrometer and liquid nitrogen cooled charge coupling device camera. Time-resolved PL measurements were obtained with a fast photomultiplier tube and digital oscilloscope in accumulation mode. The time resolution of this combination is ~ 0.8 ns. For the high-pressure PL measurements $70 \times 70 \times 30 \mu\text{m}$ samples were loaded in a gasketed

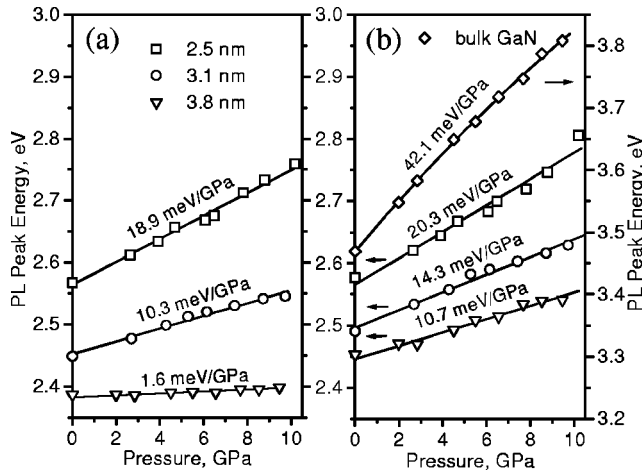


FIG. 1. Pressure dependence of the PL peaks in $\text{In}_x\text{Ga}_{1-x}\text{N}/\text{GaN}$ QWs and GaN layers at 2 W/cm^2 (a), and at 200 W/cm^2 (b) excitation intensity. Data points are fitted with straight lines for the QWs and with second-order polynomial for GaN to determine the pressure rate of change, dE/dp , shown above each line.

diamond-anvil cell filled with liquid Ar. Pressure was increased at room temperature, while all measurements were done at 35 K.

Figure 1(a) shows the pressure shift of the $\text{In}_x\text{Ga}_{1-x}\text{N}$ QW emission peak in the samples with different well width. We notice that for all well widths the QW emission peak shifts with pressure at a much smaller rate than that of GaN, shown in Fig. 1(b). We also notice that dE/dp increases from an outstandingly low value of 1.6 meV/GPa in the 3.8 nm wells to 10.3 meV/GPa in the 3.1 nm wells, and to 18.9 meV/GPa in the narrowest 2.5 nm wells. The measurements of Fig. 1(a) were obtained at a relatively low optical excitation intensity of 2 W/cm^2 . At this fluence and up to $\sim 10 \text{ W/cm}^2$ the PL peak energy did not blueshift appreciably due to the screening of built-in electric field by the photogenerated carriers. At higher excitation intensity, instead, a screening of the field results in the blueshift of the emission peaks which significantly modifies dE/dp . At the maximum excitation intensity of 200 W/cm^2 the dE/dp increases by 570% for the wide well sample, while only a 14% increase is obtained for the narrow well sample [Fig. 1(b)].

The QW PL emission decay time constants measured in a spectral interval within 20 meV from the PL peak at different pressures are shown in Fig. 2. The decay time in the 3.1- and 2.5-nm QW samples increases with pressure; the increase being more pronounced in the 3.1-nm wells structure. Decay times in the 3.8-nm wells were too long to be accurately measured with our experimental apparatus. The decay times of the $\text{In}_x\text{Ga}_{1-x}\text{N}$ samples are a measure of the radiative lifetime, which dominates over the nonradiative lifetime, as can be assessed from the invariance of the integrated PL intensity with pressure.

The behavior of the QW PL peak energy and decay time with pressure can be explained by considering that pressure changes the total strain in the QW structures and that this significantly affects F_{pz} in the wells.⁹ To determine the strain in the QWs at each pressure we add to the lattice mismatch strain a term corresponding to the elastic strain generated by

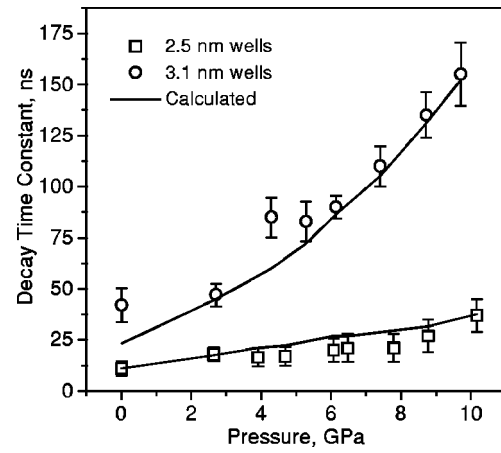


FIG. 2. Decay time constant of the QW PL as a function of applied pressure. Decay constants are obtained with a least-square single exponential fit to the measured decays. The solid lines show the carrier lifetime change with pressure calculated from the experimentally determined piezoelectric fields.

the pressure. Since the lattice mismatch between the sapphire and the GaN is accommodated by the low-temperature grown nucleation layer deposited between the GaN buffer and the substrate,^{10,11} we regard the GaN buffer as essentially stress-free before imposing the pressure. In addition, since the buffer and the GaN barriers are much thicker than the $\text{In}_x\text{Ga}_{1-x}\text{N}$ wells, the in-plane lattice mismatch is accommodated mainly by the $\text{In}_x\text{Ga}_{1-x}\text{N}$ layers. As a consequence, if we assume no plastic relaxation in the QWs, the elastic strain in the QWs without pressure is essentially determined as $\epsilon_{xx}^{mism} = (a_{\text{GaN}} - a_{\text{In}_x\text{Ga}_{1-x}\text{N}}) / a_{\text{In}_x\text{Ga}_{1-x}\text{N}}$, where $a_{\text{GaN}} = 3.189 \text{ \AA}$ and $a_{\text{In}_x\text{Ga}_{1-x}\text{N}} = 3.241 \text{ \AA}$ are the lattice constants of free-standing GaN and $\text{In}_x\text{Ga}_{1-x}\text{N}$ films.¹² In the calculation of the pressure-induced strains, however, the sapphire substrate cannot be ignored. Being the thickest element in the structures, the $30\text{-}\mu\text{m}$ -thick sapphire layer drives the changes of the in-plane strain with pressure.¹⁰ This condition determines the pressure-induced in-plane strain components $\epsilon_{xx}(p)$ and $\epsilon_{yy}(p)$ to be the same in the sapphire substrate, GaN, and $\text{In}_x\text{Ga}_{1-x}\text{N}$ layers. Assuming a quasi-hexagonal symmetry of the substrate, which is justified since $C_{14} = -23 \text{ GPa}$ is almost an order of magnitude smaller than the other elements of the stiffness tensor of sapphire,¹³ the total in-plane strain in the wells is given by

$$\begin{aligned} \epsilon_{xx}^w(p) &= \epsilon_{xx}^{mism} + \frac{C_{13} - C_{33}}{(C_{11} + C_{12})C_{33} - 2C_{13}^2} p \\ &= -0.0159 - 0.00127p, \end{aligned} \quad (3)$$

where C_{11} , C_{12} , C_{13} , and C_{33} are the elastic stiffness constants of sapphire, and p is the applied pressure in GPa. The second term in Eq. (3) is the pressure-induced in-plane strain.¹⁴ The total in-plane strain in the GaN barriers ϵ_{xx}^b is simply given by the second term in Eq. (3).

The total strain in the growth direction for the wells and GaN barriers can be obtained from the stress-strain relation considering continuity of stress $\sigma = -p$ at the interfaces between different layers.¹⁴ For the barriers we obtain

$$\varepsilon_{zz}^b(p) = \frac{-p - 2C_{13}^{\text{GaN}} \varepsilon_{xx}(p)}{C_{33}^{\text{GaN}}} = -0.00184p, \quad (4)$$

and for the $\text{In}_x\text{Ga}_{1-x}\text{N}$ wells:

$$\begin{aligned} \varepsilon_{zz}^w(p) &= -2 \frac{C_{13}^{\text{In}_x\text{Ga}_{1-x}\text{N}}}{C_{33}^{\text{In}_x\text{Ga}_{1-x}\text{N}}} \varepsilon_{xx}^{\text{mism}} - \frac{p + 2C_{13}^{\text{In}_x\text{Ga}_{1-x}\text{N}} \varepsilon_{xx}(p)}{C_{33}^{\text{In}_x\text{Ga}_{1-x}\text{N}}} \\ &= 0.00890 - 0.00198p. \end{aligned} \quad (5)$$

The terms proportional to C_{13}/C_{33} in Eqs. (4) and (5) account for the Poisson effect induced by the in-plane strain. The elastic stiffness constants of GaN and InN were taken from Refs. 15 and 16, respectively, and the $\text{In}_x\text{Ga}_{1-x}\text{N}$ constants were obtained from these values using linear interpolation. The results of the analytical calculations of strain reported here have been verified by numerical calculations with finite element method.

Using strains obtained in Eqs. (3) and (5) the $\text{In}_x\text{Ga}_{1-x}\text{N}$ band-gap change with pressure is calculated as¹⁷

$$\begin{aligned} \Delta E_g(p) &= \Delta \varepsilon_{zz}^w(p)(a_z - D_1 - D_3) + 2\Delta \varepsilon_{xx}^w(p)(a_x - D_2 - D_4) \\ &= 0.0387p \text{ [eV]}, \end{aligned} \quad (6)$$

where the deformation potentials for $\text{In}_x\text{Ga}_{1-x}\text{N}$ $a_z - D_1 = -5.80$ eV, $a_x - D_2 = -9.18$ eV, $D_3 = 5.63$ eV, and $D_4 = -2.85$ eV were found by linear interpolation between the deformation potentials of GaN and InN.¹⁷ An additional small variation of E_g with pressure comes from the pressure dependence of the electron effective mass,¹⁸ and band offsets in the wells. Considering these effects the band-gap shift of the $\text{In}_x\text{Ga}_{1-x}\text{N}$ wells is found to be $\Delta E_g(p) = 0.0382p$ eV corresponding to $dE/dp = 0.0382$ eV/GPa. Thus, in the absence of strain-dependent piezoelectric fields, dE/dp for the 15% In composition wells should not significantly vary in the different well-width samples and should be similar to that of GaN.

Next we show that the large variation of dE/dp with well width arises due to the increase of F_{pz} in the quantum wells with pressure. An increasing field results in a band-gap redshift of $\sim qF_{pz}L_w$, where q is the electron charge and L_w is the well width (quantum confined Stark effect).¹⁹ At sufficiently large electric fields and for the relatively wide wells the field almost exclusively controls the slope of the well-width dependence of the PL peak energy.^{8,20} This is the case for our samples, as can be assessed from the comparison of the linear fit to the atmospheric pressure PL (solid line in Fig. 3) with that obtained using envelope-function calculation of the QW transitions (dashed line in Fig. 3), from which the electric field is found to be ~ 1.4 MV/cm. At higher pressures where the F_{pz} is larger the accuracy of the linear fit becomes even greater.

In Fig. 4 we have plotted the variation of F_{pz} with pressure, obtained from the analysis described above. On the top axis we show the total strain in the wells produced by the applied pressure, found with Eqs. (3) and (5). F_{pz} increases from 1.4 MV/cm to 2.6 MV/cm in ~ 9 GPa. Also shown in Fig. 4 (open symbols) is F_{pz} extracted directly from the Stark shift of the QW PL peak energy with respect to the predicted bandgap behavior of $\text{In}_x\text{Ga}_{1-x}\text{N}$ calculated above [Eq. (6)].

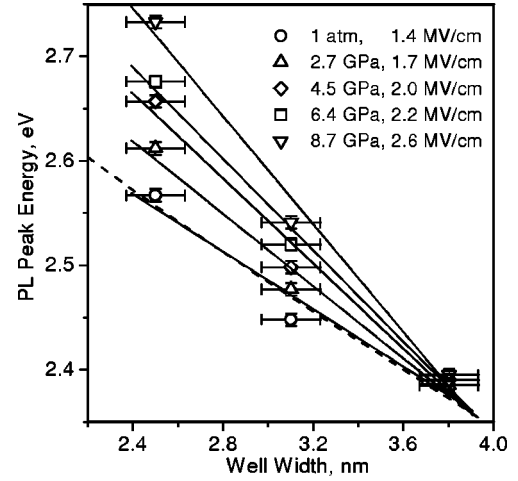


FIG. 3. PL peak energy as a function of well width at different applied pressures. The solid lines are linear fits whose slopes provide the magnitude of F_{pz} at each pressure. The dashed line is the best fit to the atmospheric pressure data obtained by calculating e_1 -hh₁ transition energy with varied transverse electric field. The field strength and energy offset were used as adjustable parameters. The best fit was obtained for $F_{pz} \approx 1.4$ MV/cm.

The agreement between the two methods is remarkable and confirms that the small dE/dp measured in $\text{In}_x\text{Ga}_{1-x}\text{N}$ QWs are due to the dramatic increase of F_{pz} with pressure. These results confirm our recent interpretation of the anomalous pressure behavior of the emission peak observed in $\text{In}_x\text{Ga}_{1-x}\text{N}/\text{GaN}$ QWs with Si-doped barriers.⁹ An increasing F_{pz} with pressure also explains the behavior of dE/dp at different excitation intensities. At high optical excitation F_{pz} in the wells is partially screened out by the large density of photogenerated carriers, and thus the Stark shift of the PL

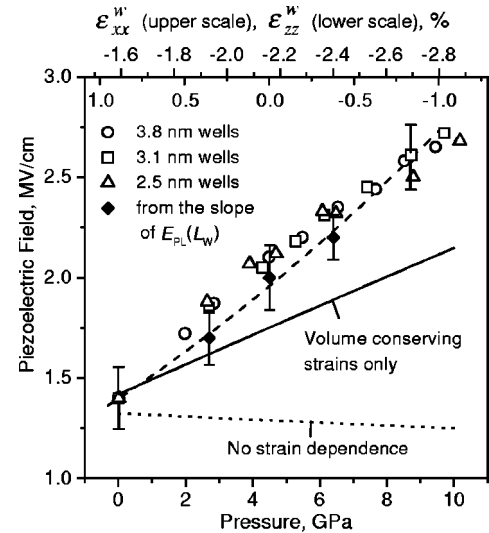


FIG. 4. Pressure dependence of F_{pz} in quantum wells. Dotted line—calculated assuming no strain dependence of piezoelectric constants; solid line—calculated considering only the deviatoric strain dependence of the constants given in Ref. 6; solid diamonds—data of Fig. 3 (dashed line is a polynomial fit to the data points); open symbols—obtained from the Stark shift of PL peaks.

peak energy is smaller compared to that in the low excitation regime, leading to a larger dE/dp . Because the Stark shift is well-width dependent, the changes in dE/dp with excitation intensity are more significant in the wider wells than in the narrower wells. The increase in dE/dp with excitation follows the nearly quadratic dependence of the Stark shift on the electric field.¹⁹

The increase of F_{pz} also explains the increase in the PL decay time with pressure. Using the values of F_{pz} of Fig. 4 we calculated the variation of the carrier lifetime with pressure for the QWs of different widths. The radiative lifetime was found as the inverse of the square of the electron-hole wave-function overlap in the wells with applied transverse electric field. The results of this calculation normalized to the value of the decay time measured in the 2.5 nm well at atmospheric pressure are shown by the solid line in Fig. 2. Excellent agreement is obtained between the experimentally measured decays and the calculated lifetime. The carrier lifetime behavior in the QW samples contrasts with that measured in an unstrained thick $\text{In}_x\text{Ga}_{1-x}\text{N}$ epilayer, where the lifetime is found to slightly decrease with pressure.⁹

To investigate the origin of the increase in F_{pz} with pressure we calculated the field for two conditions: (a) strain-independent piezoelectric constants, and (b) deviatoric strain dependent piezoelectric constants. The F_{pz} was calculated as¹

$$F_{pz} = L_b(P_b - P_w)/(L_b\epsilon_w + L_w\epsilon_b), \quad (7)$$

where $\epsilon_{w,b}$ are the permittivities of the $\text{In}_x\text{Ga}_{1-x}\text{N}$ well and GaN barrier, and $L_{w,b}$ are the well and the barrier widths. The piezoelectric polarizations in the well and in the barrier are found as

$$P_{w,b} = e_{33}^{w,b}\epsilon_{zz}^{w,b}(p) + 2e_{31}^{w,b}\epsilon_{xx}^{w,b}(p). \quad (8)$$

The resulting variation of F_{pz} for the 3.1 nm wells for $e_{33}^{w,b} = 0.63 \text{ C/m}^2$ and $e_{31}^{w,b} = -0.32 \text{ C/m}^2$ (Ref. 6) for case (a) is shown by the dotted line in Fig. 4. This calculation shows that if strain does not affect the piezoelectric constants, F_{pz} would slightly decrease with pressure. We therefore conclude that the only way to reproduce the experimentally observed

pressure dependence of the field is by considering a strong dependence of the piezoelectric constants on strain, i.e., a nonlinear piezoelectric effect. We then calculated the changes in F_{pz} that arise from changes of piezoelectric constants with deviatoric strain. We use the strain dependence of the piezoelectric constants of GaN given in Ref. 6 both for the GaN barriers and $\text{In}_x\text{Ga}_{1-x}\text{N}$ wells, as the dependence of the piezoelectric constants in $\text{In}_x\text{Ga}_{1-x}\text{N}$ on strain is not available. The piezoelectric field obtained in this way is shown by the solid line in Fig. 4. Although F_{pz} in this case significantly increases with pressure it falls short of the experimental values. This result clearly shows that dilatational, as well as deviatoric strain, significantly affect the piezoelectric response of $\text{In}_x\text{Ga}_{1-x}\text{N}/\text{GaN}$ QWs.

The modification of the piezoelectric constants with strain revealed from these experiments is also present in $\text{In}_x\text{Ga}_{1-x}\text{N}/\text{GaN}$ QWs in the absence of pressure, due to the lattice mismatch strain. While the in-plane strain components ϵ_{xx} in both cases are comparable in the typical range of indium compositions of 10–20 %, the strain generated by the lattice mismatch in the growth direction ϵ_{zz} has a positive sign, as opposed to the strain produced by the pressure (Fig. 4). This difference affects the relative contribution of the deviatoric and dilatational components of strain, and therefore the specific strain dependence of the piezoelectric field, which still awaits its investigation.

In conclusion, we have determined the piezoelectric field in $\text{In}_x\text{Ga}_{1-x}\text{N}/\text{GaN}$ quantum wells of different width for different strain conditions. An almost twofold increase of the piezoelectric field in $\sim 9 \text{ GPa}$ is shown to be the result of the strong dependence of the piezoelectric constants with total strain, i.e., nonlinear piezoelectric effect. We show that both, dilatational and deviatoric strain components, contribute to such effect.

The CSU group gratefully acknowledges the support of the National Science Foundation and the Colorado Photonics and Optoelectronics Program.

-
- ¹V. Fiorentini *et al.*, Phys. Rev. B **60**, 8849 (1999).
²C. Wetzel, T. Takeuchi, H. Amano, and I. Akasaki, Phys. Rev. B **61**, 2159 (2000).
³T. Takeuchi *et al.*, Jpn. J. Appl. Phys., Part 2 **36**, L382 (1997).
⁴A. D. Bykhovski, B. L. Gelmont, and M. S. Shur, J. Appl. Phys. **81**, 6332 (1997).
⁵A. Dal Corso, M. Posternak, R. Resta, and A. Baldereschi, Phys. Rev. B **50**, 10 715 (1994).
⁶K. Shimada, T. Sota, K. Suzuki, and H. Okumura, Jpn. J. Appl. Phys., Part 2 **37**, L1421 (1998).
⁷We define dilatational (volumetric) strain components: $\epsilon_{ij}^{\text{dil}} = 1/3(\epsilon_{xx} + \epsilon_{yy} + \epsilon_{zz})\delta_{ij}$, and deviatoric (volume conserving) components: $\epsilon_{ij}^{\text{dev}} = \epsilon_{ij} - \epsilon_{ij}^{\text{dil}}$, where i and j identify the principal axes, and $\delta_{ij} = 1$ if $i = j$, and $\delta_{ij} = 0$ if $i \neq j$.
⁸R. André *et al.*, Phys. Rev. B **53**, 6951 (1996).
⁹G. Vaschenko *et al.*, Appl. Phys. Lett. **78**, 640 (2001).
¹⁰P. Perlin *et al.*, Jpn. J. Appl. Phys., Part 1 **85**, 2385 (1999).
¹¹L. T. Romano *et al.*, J. Appl. Phys. **87**, 7745 (2000).
¹²M. Leszczynski, T. Suski, J. Domagala, and P. Prystawko, in *Properties, Processing and Applications of Gallium Nitride and Related Semiconductors*, edited by J. H. Edgar *et al.* (INSPEC, London, 1999), p. 6.
¹³Y. Takeda and M. Tabuchi, *ibid.*, p. 381.
¹⁴Details of the strain calculations using the linear approximation of elasticity theory will be published elsewhere.
¹⁵A. Polian, M. Grimsditch, and I. Grzegory, J. Appl. Phys. **79**, 3343 (1996).
¹⁶A. F. Wright, J. Appl. Phys. **82**, 2833 (1997).
¹⁷W. W. Chow and S. W. Koch, *Semiconductor-Laser Fundamentals* (Springer, Berlin, 1999), p. 189.
¹⁸P. Perlin *et al.*, Appl. Phys. Lett. **70**, 2993 (1997).
¹⁹G. Bastard, E. E. Mendez, L. L. Chang, and L. Esaki, Phys. Rev. B **28**, 3241 (1983).
²⁰M. Leroux *et al.*, Phys. Rev. B **60**, 1496 (1999).